MEASUREMENT SCIENCE REVIEW, **21**, (2021), No. 6, 180-184

sciendo

ISSN 1335-8871

MEASUREMENT SCIENCE REVIEW

Phase Variation Measurement in Mach–Zehnder Interferometric Switch

Sichen Fan[1,2,3], Jun Ruan[1,3], Dandan Liu[1,3], Xinliang Wang[1,3], Fan Yang[1,2,3], Yong Guan[1,3], Hui Zhang[1,2,3], Junru Shi[1,2,3], Yang Bai[1,2,3], Shougang Zhang[1,3]

[1]*National Time Service Center, Chinese Academy of Science, Xi'an, Shaanxi, 710600, China, ruanjun@ntsc.ac.cn*
[2]*University of Chinese Academy of Science, Beijing 100039, China*
[3]*Key Laboratory of Time and Frequency Primary Standards, Chinese Academy of Science, Xi'an, Shaanxi, 710600, China*

Phase variations of the interrogation field lead to frequency shifts in Ramsey-type atomic clocks. This paper reports the development of a 300 MHz Mach–Zehnder (MZ) switch that effectively suppresses phase-transient effects. Similar to MZ interferometers, this radio-frequency (RF) MZ switch comprises two arms that are power- and phase-matched with each other. By inserting a PIN diode RF switch in one arm, the other arm remains undisturbed, freeing it of the phase transient. Trigger phase fluctuation measurements are implemented by using a lock-in amplifier to extract the in-phase and quadrature (I/Q) demodulation data. The results show that the extinction ratio of the RF MZ switch phase fluctuations is <5 µrad, which is significantly lower than that of a PIN (50 µrad). When applied to a cesium fountain clock, the RF MZ switch produces a frequency shift better than 1.73×10^{-16}.

Keywords: Phase variations, Mach-Zehnder switch, trigger phase fluctuation measurements, cesium fountain clock, frequency shift.

1. INTRODUCTION

Radio-frequency (RF) radiation is widely used in radar, communications, and microwave measurements [1]-[2]. RF switches are among the important components of microwave control circuits, and a variety of specifications and forms of packaging of PIN diodes suitable for use as such switches are available. In studies of RF switches, the focus has generally been on bandwidth, insertion loss, isolation, and power. However, few studies have paid attention to the phase transients that occur when a switch is on. Ramsey interrogation, first developed by Norman Ramsey [3]-[5], has been applied to atomic or molecular beams interacting with spatially separated fields. It has also been applied to trapped atoms or ions at the same location with a field that is switched on and off in a time sequence. The phase variation $\Delta\phi$ (in rad) between two Ramsey interactions of duration τ shifts the frequency of an atomic clock by $\Delta\nu = \Delta\phi/2\pi T$ (in Hz), where T is the Ramsey interrogation time. As commercial microwave switches inherently exhibit phase transients at levels of 50 µrad, they cannot be applied to the direct amplitude control of a Ramsey interrogation microwave field. For example, a relatively small 10 µrad phase difference at 9 192 631 770 Hz leads to a fractional frequency offset of 3×10^{-16} in a cesium fountain clock (for which typically T = 0.5 s). Moreover, phase transient usually leads to this frequency offset, unstable due to fluctuation of temperature, which will degrade the long term frequency stability.

This paper presents an RF Mach-Zehnder (MZ) interferometric switch that suppresses large phase transients. In Section 2, a highly sensitive trigger phase analyzer is introduced, with a resolution of 2 µrad at an integration time of 10^5 s. In Section 3, the setup of the RF MZ switch is outlined, and the measurements on the switch are described. Conclusions are given in Section 4.

2. MEASUREMENT OF PHASE FLUCTUATIONS

To analyze the phase transients of a radio-frequency signal when the switch is on, a triggered-phase transient analyzer (TPTA) with resolution of 2 µrad has been developed. Santarelli et al. [6] at the Laboratoire National de Métrologie et d'Essais—Systèmes de Référence Temps-Espace (LNE-SYRTE) built a trigger phase analyzer with digital in-phase and quadrature (I/Q) demodulator and single-value decomposition to extract the phase from a microwave signal. Kazda et al. [7] at the Physikalisch-Technische Bundesanstalt (PTB) developed a phase analyzer system utilizing a commercially available field-programmable gate array (FPGA) to implement I/Q demodulation. Alternatively, a commercial lock-in amplifier can be used to generate the I/Q demodulation data, which can then be collected by a triggered analog-to-digital (A/D) card to calculate the phase value.

DOI: 10.2478/msr-2021-0024

To analyze the signal phase of the device under test (DUT), it is first necessary to down-convert from the radio domain (f_{DUT}) to the kilohertz frequency range (f_{diff}). The transient phase data are extracted through comparison with another continuous signal (f_{signal}) from a commercial lock-in amplifier at the same frequency f_{diff}. The pulse signal and the continuous signal can be expressed as

$$\begin{cases} u_1(t) = v_1 \sin[2\pi f_{diff} t + \theta_1(t)], \\ u_2(t) = v_2 \sin[2\pi f_{signal} t + \theta_2(t)]. \end{cases} \quad (1)$$

After the two signals have been mixed, the signal output from the mixer can be expressed as

$$\begin{aligned} u_3(t) &= K u_1(t) u_2(t) \\ &= v' \sin[2\pi f_{diff} t + \theta_1(t)] \sin[2\pi f_{signal} t + \theta_2(t)] \\ &= -\tfrac{1}{2} v' \{\cos[2\pi (f_{diff} + f_{signal}) t + \theta_1(t) + \theta_2(t)] \\ &\quad - \cos[2\pi (f_{diff} - f_{signal}) t + \theta_1(t) - \theta_2(t)]\}. \end{aligned} \quad (2)$$

The high-frequency component of the signal is removed by low-pass filtering, and the low-frequency component is then obtained as

$$u_3(t) = \tfrac{1}{2} v' \cos[2\pi (f_{diff} - f_{signal}) t + \theta_1(t) - \theta_2(t)]. \quad (3)$$

When $f_{diff} = f_{signal}$, the low-frequency component of the signal is given by

$$u_X(t) = \tfrac{1}{2} v' \cos[\theta_1(t) - \theta_2(t)]. \quad (4)$$

Subsequently, the reference signal is shifted by -90° to give an output

$$\begin{aligned} u_Y(t) &= \tfrac{1}{2} v' \cos[\theta_1(t) - \theta_2(t) - \tfrac{\pi}{2}] \\ &= \tfrac{1}{2} v' \sin[\theta_1(t) - \theta_2(t)]. \end{aligned} \quad (5)$$

The signal u_N can then be divided by the signal u_M, allowing the phase difference to be obtained as

$$\theta_1(t) - \theta_2(t) = \arctan\left(\frac{u_Y}{u_X}\right). \quad (6)$$

A phase fluctuation measurement system was built according to this principle, as shown in Fig.1. The measured signal, reference signal, and sampling clock signal are all locked to the 10 MHz of the commercial signal source (DS345 from Stanford Research Systems). The first signal source, which is dual-channel, generates 300 MHz of DUT; the 300.01 MHz signal is taken as the reference signal. Through mixing, the 10 kHz signal of the frequency offset, f_{diff}, is connected to an SR830 lock-in amplifier through the terminal that is to be tested. The second source generates a 10 kHz signal that is linked to the reference input of the SR830 amplifier. The two output signals of the SR830 amplifier (X and Y) are collected into memory through the peripheral component interconnect (PCI) data card. Finally, the data are analyzed by a computer. Simultaneously, the third signal source provides the trigger signals of the PCI data acquisition card and the switch. In this system, a PCI-6122 synchronous sampling card (from National Instruments) is used as the acquisition board, with 16-bit precision and a 500 kS/s sampling rate.

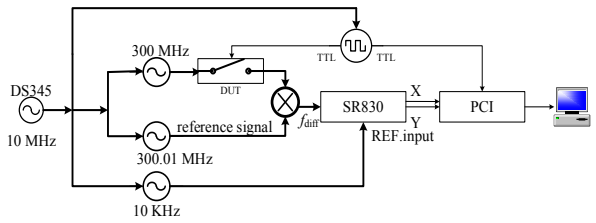

Fig.1. Structure of the phase fluctuation measurement system.

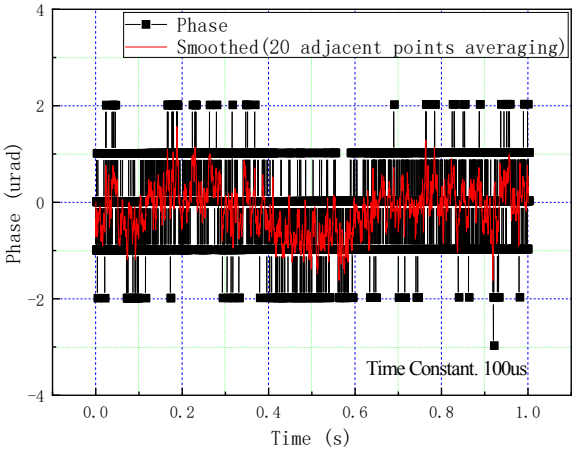

a)

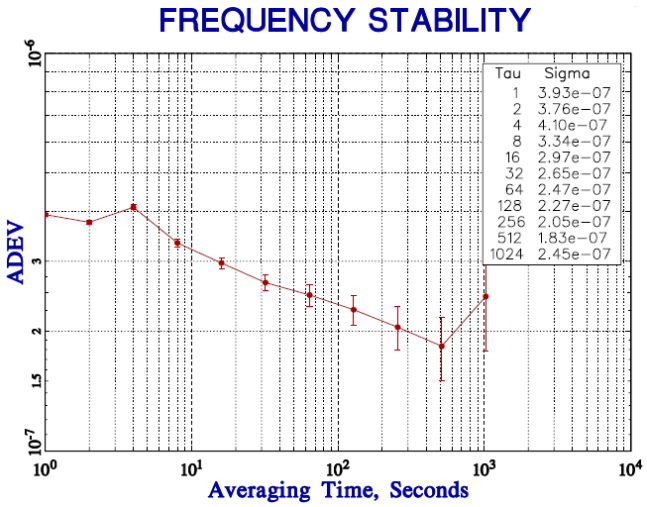

b)

Fig.2. a) Phase fluctuations of the background: the black line shows actual measurement data and the red line shows data smoothed by 20-adjacent-points averaging. b) Allan variance of the average phase of each cycle (in the absence of a switch).

First, the phase fluctuations of the background in the absence of a switch were measured, as shown in Fig.2.a). The phase fluctuation of the system itself was ~2 μrad. The frequency shift resulting from this was approximately 6.93×10^{-17}. Fig.2.b) shows the Allan variance of the average phase of each cycle.

Three widely used commercial microwave switches, ZMSW-1211, F192A, and SHX801, were each connected to the 300 MHz output for measurement. The data acquisition card was configured for rising edge acquisition. Fig.3. shows the phase fluctuation measurement results (for a time constant of 100 μs). There was a huge phase transient when the switch was turned on. This may be due to the thermal effect of the switch. The ZMSW-1211 and F192A switches both contain PIN diodes. Carrier recombination generates heat inside the diode, as a result of which the internal current changes more rapidly. There is therefore a sudden rise in the internal temperature of the device, leading to a very severe change. SHX801 is a TTL trigger-type mechanical switch, with its state controlled by an electromagnet, which generates high power. When the switch is turned on, the thermal effect increases the strength of the phase fluctuations. After a while, the heat gradually decreases, meaning that the phase gradually becomes flat.

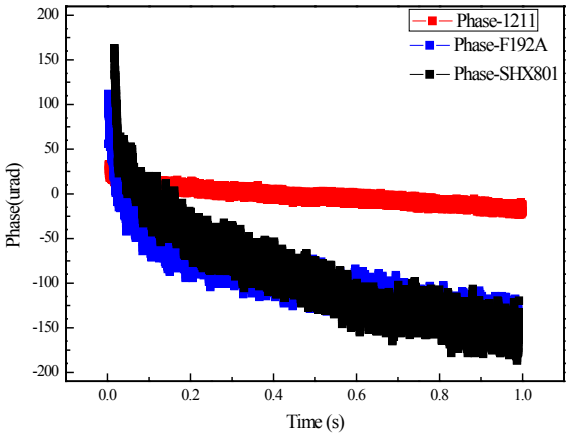

Fig.3. Phase fluctuations of three commercial switches: ZMSW-1211 (red), F192A (blue), and SHX801 (black).

The ZMSW-1211 switch showed the best performance among the three commercial switches. However, it still exhibited a large phase transient, which is noticeable because this would lead to an increase in the frequency shift of a cesium atomic fountain clock. The phase fluctuations were tested for different time constants, and it was found that the larger the time constant, the more stable was the output, but the slower was the response. When the time constant was in the range from 100 μs to 1 ms, phase transients were clearly manifested by all three of the commercial switches. The switch labeled SHX801 is a kind of mechanical RF switch and the other two are PIN diode switches which belong to non-reflective (F192A) and reflective (ZMSW-1211) SPST switch. When the switch is on, the energy accumulated inside the switch package due to the high resistance will decrease largely, which means the phase diminution of transmitted signals decreasing due to temperature reduction. In general, the phase transient is inevitable when the switch is on.

3. RADIO-FREQUENCY MACH–ZEHNDER SWITCH

A transient-less RF switch comprises a MZ interferometer into one arm of which a diode RF switch is inserted [8]-[10]. If the lower arm of the MZ switch is tuned to a dark fringe configuration when the PIN switch is on, the MZ switch output is zero by a destructive interference. The output will be the same as the signal of the Upper arm, which has the status of on when the PIN switch is off. In other words, the RF MZ switch is off when PIN switch is on. Otherwise, the RF MZ switch is on when PIN switch is off. As a result, the RF signal is unperturbed in the Upper arm when the diode switch is off in the Lower arm. In this way, the RF MZ switch effectively suppresses phase-transient effects.

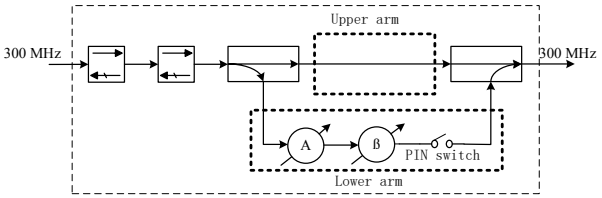

Fig.4. Schematic of the RF MZ switch.

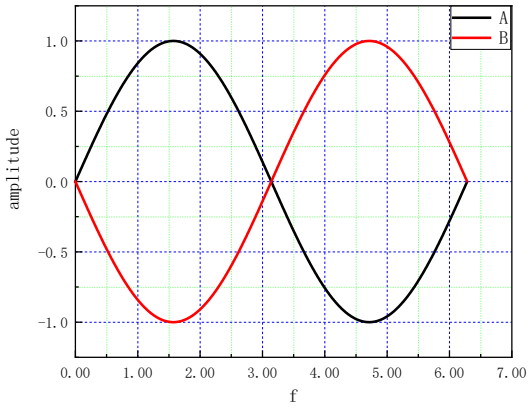

Fig.5. Principle of RF MZ switch.

Fig.4. illustrates the implementation of the RF MZ switch. The 300 MHz signal passes through two isolators and is then split into two paths using a directional coupler (with coupling 10 dB). Here, two microwave isolators are used to improve isolation and impedance matching. The output port is connected directly to the coupled port of the other directional coupler. The coupled port is connected with an adjustable attenuator(A) and an adjustable phase shifter(β). It is then linked to a commercial microwave switch. Finally, the signal is connected with the output port of the other directional coupler. In this way, the two signals are combined into one signal by a directional coupler. The phase of one arm relative to the other is coarsely adjusted by the cable length. The phase shifter and attenuator are used to finely adjust the phase and power of the MZ switch to the minimum value, as shown in Fig.5.

The phase fluctuations of the RF MZ switch were analyzed using the TPTA. The DUT of the TPTA described in Section 2 was replaced by the RF MZ switch based on ZMSW-1211. As shown in Fig.3., commercial RF switches exhibit large phase transients of approximately 50 µrad, and these transients are obvious when the switch is on. However, when the RF MZ switch was used instead of a commercial switch, the phase transients were effectively suppressed, as shown in Fig.6. According to the expression $\Delta v = \Delta\Phi/2\pi T$, the resulting frequency shift was $<1.73 \times 10^{-16}$ when the phase fluctuation of the RF MZ switch was <5 µrad.

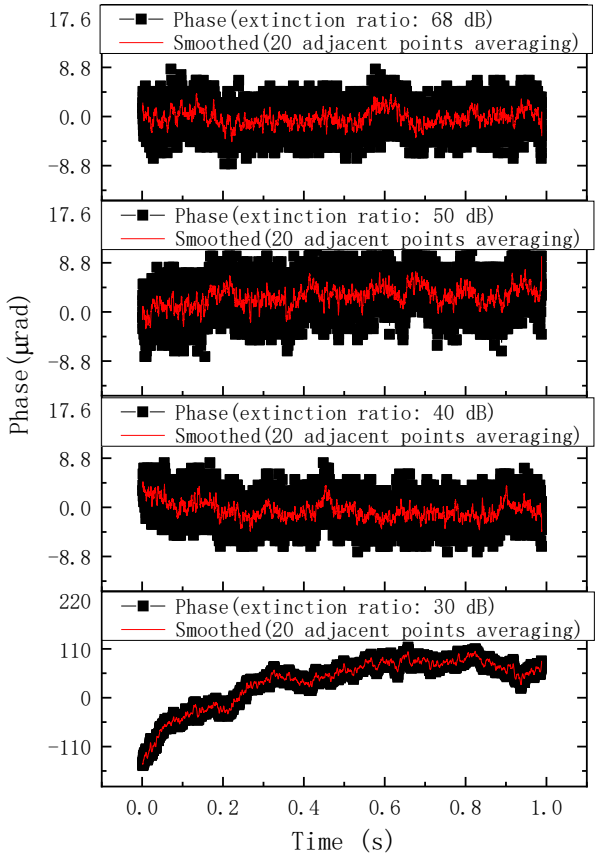

Fig.6. Phase fluctuations at different extinction ratios: the black lines show actual measurement data, and the red lines are smoothed by 20-adjacent-points averaging.

Phase fluctuations with different extinction ratios were studied by adjusting the attenuator. First, the extinction ratio of the interference switch was adjusted to be as large as possible, to remove phase transients, by using the phase shifter and the attenuator. Then, the extinction ratio was gradually reduced using the attenuator. Fig.6. shows the phase fluctuations at different extinction ratios. With a 5 µrad phase fluctuation and an extinction ratio of 68 dB, the frequency shift was $<1.73 \times 10^{-16}$, and this was also the same when the extinction ratio was 50 dB. Similarly, when the phase fluctuation was ~10 µrad and the extinction ratio was 40 dB, the frequency shift was 3.46×10^{-16}. There was a slight phase transient at this time. There was also an obvious phase transient at an extinction ratio of 30 dB. To maintain the frequency shift at a level of the order of 10^{-16}, the extinction ratio of the interference switch should be >50 dB.

Finally, an initial analysis of the relationship between the temperature and the extinction ratio of the RF MZ switch was performed. The extinction ratio of the RF MZ switch was measured at different temperatures. First, the interference switch was adjusted to be >60 dB, and it was then placed into a temperature-control box. The extinction ratios of the interference switch and the temperature in the box were measured simultaneously. It is worth noting that it was necessary to preheat the devices in the box each time the temperature was changed.

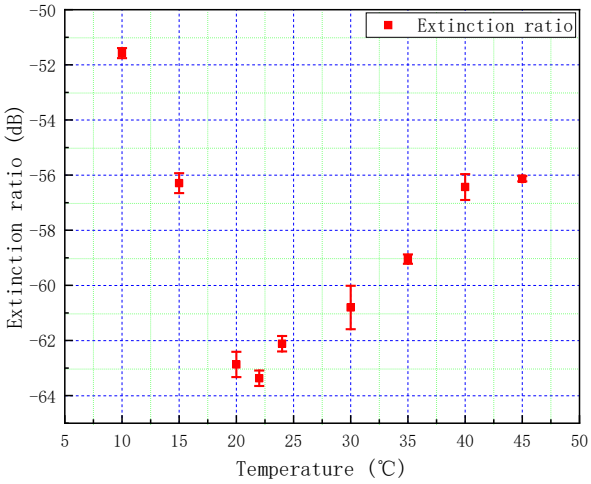

Fig.7. Effect of temperature on the extinction ratio of the interference switch: the black line shows the current temperature, and the red line shows the extinction ratio.

Fig.7. shows the variation in the extinction ratio as the temperature inside the box is increased. The extinction ratio of the RF MZ switch showed a trend of first decreasing and then increasing as the temperature was gradually increased from 10°C to 45°C. When the temperature changes, the phase changes. At this time, the phases of the two arms do not match, causing the extinction ratio to drop. However, the extinction ratio still remained above >50 dB, and the frequency shift caused by the RF MZ switch was $<10^{-16}$.

4. Conclusions

A 300 MHz MZ switch was developed based on an optical MZ interferometer. To analyze its phase transients, TPTA was implemented at a microradian resolution. As shown by the TPTA, the phase fluctuations of the RF MZ switch were better than 5 µrad over 10 h, resulting in a frequency shift of $<1.73 \times 10^{-16}$. Phase fluctuations were also examined at different extinction ratios, and it was found that the phase fluctuations increased as the extinction ratio decreased. The relationship between temperature and the extinction ratio of the RF MZ switch was also analyzed in a temperature-control box. The results show that temperature has a great influence on RF MZ switches, owing to their sensitivity to cable length. However, the RF MZ switch, when applied to a fountain clock, will limit this frequency shift to $<10^{-16}$. To

improve the performance of RF MZ switches, lower-drift attenuators and better temperature control measures are necessary.

ACKNOWLEDGMENT

This research was supported financially by Chinese Academy of Sciences for Western Young Scholars (XAB2018A06, XAB2019A07), Large Research Infrastructures Improvement Funds of Chines Academy of Sciences(DSS-WXGZ-2020-0005).

REFERENCES

[1] Putnam, J., Barter, M., Wood, K., Leblanc, J. (1997). A monolithic GaAs PIN switch network for a 77 GHz automotive collision warning radar. In *1997 IEEE MTT-S International Microwave Symposium Digest*. IEEE, vol. 2, 753-756.

[2] Gu, Z., Johnson, D., Belletete, S., Fryklund, D. (2004). Low insertion loss and high linearity PHEMT SPDT and SP3T switch ICs for WLAN 802.11 a/b/g applications. In *IEEE Symposium on Radio Frequency Integrated Circuits (RFIC)*. IEEE, 505-508.

[3] Ramsey, N.F. (1958). Molecular beam resonances in oscillatory fields of nonuniform amplitudes and phases. In *Physical Review*, 109 (3), 822-825.

[4] Ramsey, N.F. (1950). A molecular beam resonance method with separated oscillating fields. In *Physical Review*, 78 (6), 695-698.

[5] Ramsey, N.F. (1956). *Molecular Beams*. Oxford: Clarendon Press.

[6] Santarelli, G., Governator, G., Chambon, D., Lours, M., Rosenbusch, P., Guéna, J., Chapelet, F., Sébastien, B., Michael, E.T., Laurent, P., Potier, T., Andre, C. (2009). Switching atomic fountain clock microwave interrogation signal and high-resolution phase measurements. In *IEEE Transactions on Ultrasonics, Ferroelectrics, and Frequency Control*, 56 (7), 1319-1326.

[7] Kazda, M., Gerginov, V., Huntemann, N., Lipphardt, B., Weyers, S. (2016). Phase analysis for frequency standards in the microwave and optical domains. *IEEE Transactions on Ultrasonics, Ferroelectrics, and Frequency Control*, 63 (7), 970-974.

[8] Santarelli, G., Governatori, G., Lours, M., Chambon, D., Clairon, A. (2006). Phase transient measurement at the micro radian level for atomic fountain clocks. In *Proceedings of the 20th European Frequency and Time Forum*. IEEE, 166-172.

[9] Yu, X., Shum, P., Dong, X. (2006). Photonic-crystal-fiber-based Mach–Zehnder interferometer using long-period gratings. In *Microwave and Optical Technology Letters*, 48 (7), 1379-1383.

[10] Bucaro, J.A., Dardy, H.D., Carome, E.F. (1977). Optical fiber acoustic sensor. In *Applied Optics*, 16 (7), 1761-1762.

Received July 11, 2021
Accepted September 30, 2021